PREFACE Milestone Report

Milestone#: MS45

Milestone name: Pelagic fish and prey field dynamics in their habitat – report

WP#: WP12

Lead beneficiary: IRD

Delivery date from annex I: 31.10.2017 (Actual achievement date: 24.4.2018)

Milestone achieved: YES

Comments: This report incorporates work achieved earlier under D12.2 and MS42, and together with D12.3&D12.4, summarizes the analyses carried out in PREFACE for the tropical and subtropical eastern Central Atlantic in WP12.

PREFACE MS45 report: pelagic fish and prey field dynamics in their habitat

Synthesis of pelagic fish and prey field dynamics in combination with abiotic and biotic data of their habitat [link with CT2 and MS42]

Patrice Brehmer, IRD, Brest, France

Ivanice Monteiro, INDP, Mindelo, Cabo Verde

Pericles da Silva, INDP, Mindelo, Cabo Verde

Stephanie Czudaj, Thünen Institute, Hamburg, Germany

Ismael Nunez-Riboni, Thünen Institute, Hamburg, Germany

Matthias Schaber, Thünen Institute , Hamburg, Germany

Heino O. Fock, Thünen Insitute, Hamburg, Germany

Table of contents

Overall introduction

This milestone report contains an update on the analysis of Yellowfin tuna (YFT) bioclimatic modelling as well as the synthesis based on D12.2 and MS42.

Catch opportunities of Yellowfin tuna (*Thununnus albacares*) in the waters of Cape Verde

Abstract

Local Yellowfin tuna (*Thunnus albacares*, YFT) catch rates covering the area 10-20°N latitude and 10-30°W longitude were analysed to indicate catch opportunities in Cape Verde waters. Local catch-per-unit-effort ($CPUE_l$) is treated as a function of stock size, N_s, and environmental factors, V_i, the latter at local scale or at stock scale in terms of climate indices. Of the two indices applied to indicate stock size, *i.e*. the Japanese long line stock index (LLindex) and the so-called Index4 series, the LLindex.

All models are wrong, but some are useful.

George Box, 1978

Introduction

Yellowfin tuna (*Thunnus albacares*, YFT) is a temperate-tropical species distributed mainly in the epipelagic oceanic waters of the three oceans (Arrizabalaga *et al.*, 2015). The sizes exploited range from 30 cm to over 170 cm; maturity occurs at about 100 cm. In the Atlantic, YFT migrate seasonally avoiding areas of lower sea surface temperature (SST). YFT undertake extensive migrations. In the Atlantic, high YFT catches are obtained in the eastern tropical Atlantic in quarters 2, 3, and 4, catches, with increasing catches also around Cape Verde. In the first two quarters of the year, YFT mainly aggregate in the equatorial Atlantic and the Gulf of Guinea, one of the main spawning areas. Juvenile YFT extend their habitat into the western subtropical Atlantic up to the Gulf of Maine (Fonteneau and Soubrier, 1996). In an analysis of tuna habitat requirements at global scale, Arrizabalaga et al. (2015) showed that YFT had very specific habitat needs with a preference for warm surface waters > 24°C. Highest catch rates of YFT in the tropical Atlantic are linked to water temperatures of 24-25°C. For the North Atlantic, Lan et al. (2011) analysed a short time series 1998-2007 based on Taiwanese long-line fisheries data in relation to the North Atlantic Tropical index (NTA), sea surface temperature (SST), subsurface temperature, chlorophyll a concentration, net primary productivity, and wind speed. For the fleet considered, subsurface temperature was an important determinant of YFT catch rates.

YFT fisheries is mainly conducted by means of long-lining and purse seining. In the case of artisanal fisheries, hand lining is also applied. In Cape Verde waters, annual total catch in terms of landings is about 10000 t (Stobberup *et al.*, 2005). YFT contributed some 20 % of the total landings, but has in declined in abundance as evidenced in a GLM analysis of surveys from 1964 to 1994 (Stobberup *et al.*, 2005). This may be related to the trend in Atlantic stock size. In contrast to the increasing catches of YFT in other oceans, there has been a steady decline in overall Atlantic catches, with an overall decline of 45% since the

peak catches of 1990 (Anonymous, 2011). The catches from surface fisheries (Purse seining) in the Atlantic Ocean decreased between 2001 and 2004, whereas LL catches increased. After 2006, the catches of the LL fishery declined, although some surface fisheries increased in the eastern Atlantic.

Assessments indicate that YFT total stock abundance has decreased from a very high level in the 1960's until the early 2000's but is recovering since then. At present, biomass appears to be at maximum sustainable yield-level (MSY), offering good prospects for future fisheries (Anonymous, 2016). The stock encompasses all Atlantic YFT, not only the part accessible in Cape Verde waters.

In order to meet requirements of the ecosystem approach to fisheries management at local scale, further investigations are necessary to analyse catch opportunities in relation to environmental factors and climate change at a regional scale (e.g. Lan *et al.*, 2013). In the Atlantic, catch opportunities off NE Brazil (Zagaglia *et al.*, 2004) and along tracks of drifting fish attracting devices (Lopez *et al.*, 2017) indicated the importance of ocean productivity, mixed layer depth and the position of the Intertropical Convergence Zone (ITCZ). We aim at analysing catch opportunities in the waters around Cape Verde, subject to both artisanal and industrial/semi-industrial fishing by domestic and international fleets. Fisheries-independent abundance data are not available, and only information comes from opportunistic fisheries targeting tuna aggregations (Watson and Kerstetter, 2006). The fisheries operates at high technological skills in terms of fleet communication, utilization of satellite imagery and aircraft to detect fronts and near-surface schools, and other electronic devices to minimize the risk of unsuccessful fishing effort.

Material and Methods

Rationale

The most simple model for commercial data is a linear – usually spatially stratified - relationship between catch-per-unit-effort (CPUE, C/E) and stock abundance N_s and catchability q, where fisheries is unconstrained to maintain a direct proportionality between stock and CPUE (Hilborn and Walters, 1992).

$$C_s/E_s=qN_s \qquad \text{Eq. 1}$$

Two concepts exist for the relationship between local abundance and total stock (Fonteneau and Soubrier, 1996), *i.e.* the pipeline-model with a permanent flow from total stock into a local population, and the concept of local populations with temporarily constrained exchange. Hence, local catch-per-unit-effort ($CPUE_l$) is treated as a function of stock size and environmental factors, V_i, either in terms of a pipeline model according to Eq. 2b or in a specification according to Eq. 2a. Eq. 2b would derive from Eq. 1 by taking the log's and implying an exponential relationship for environmental factors at stock scale. The rationale for Eq. 2a is that $CPUE_l$, *i.e.* at local scale, not necessarily has a log

relationship to N_s and could be more dependent on extreme values than on the mean state.

Log-transformed $CPUE_l$ values were used to meet the normality criterion for linear models (Zuur *et al.*, 2010) and to account for log-normal errors (Maunder and Punt, 2004).

$$\ln(CPUE_l) \sim f(N_s) + \Sigma f(V_i) + \varepsilon \qquad \text{Eq. 2a}$$

$$\ln(CPUE_l) \sim f(\log(N_s)) + \Sigma f(V_i) + \varepsilon \qquad \text{Eq. 2b}$$

Objective factors that affect the use of commercial data are changes in fleet efficiency, shifts in target species, environmental factors and fleet dynamics (Maunder and Punt, 2004; Maunder *et al.*, 2006). Hilborn and Walters (1992) further indicate subjective factors related to fishermen's behaviour with a significant effect on local CPUE: efficiency of search and interaction between fishermen, and depletion of the fish stock at local scales. Fisheries dependent data only disclose the part of the stock that was fished above an economic threshold, knowledge on the stock at low abundances cannot be obtained from commercial data (Fig. 1). A natural factor that affects CPUE dynamics lies in the distribution of fish, *e.g*. fish school tend to have consistent high CPUE even at low stock sizes, and how the stock is related to local abundance. For YFT, a pattern of diffusive movements within favourable habitats is known, indicating a moderate level of aggregation, and advective movements, when long-distance migrations take place (Fonteneau and Soubrier, 1996).

To account for these sources of uncertainty, we choose a multiple approach with up to 16 model specifications based on contrasting hypotheses (see Table 1)(Burnham and Anderson, 2004). Using Goodness-of-fit criteria, we applied linear modelling rather than non-parametric approaches to distinguish between contrasting functional relationships in relation to the underlying assumptions Table1).

Yellowfin tuna stock and environmental Input variables

Yellowfin tuna stock indices

Two indices were applied; the Japanese long line stock index (LLindex) and the so-called Index4 series.

The Japanese LL stock index (LLindex) as revised by the ICCAT YFT Species Group has the advantage of long duration and extensive spatial coverage. However, there is a noted shift in targeting from YFT before 1975, to BET after 1976. This change in targeting was likely accompanied by changes in gear configuration and/or fishing operations, but data describing gear configuration are not available to directly quantify the change in targeting. The ICCAT assessment group recommends to include this index in all stock assessment models 1976-2014 (Anonymous, 2016).

The Index4 series as from 2011, is a combined index using a GLM approach with the following model formulation (Anonymous, 2011):

$$\ln(\text{Index4}) \sim \text{year}_i + \text{fleet}_j + \varepsilon_i \qquad \text{Eq. 3}$$

Index4 combines different fleets from different countries, i.e. purse seine fisheries data, catches obtained at Fish-Attracting-Devices, and long line fisheries data.

Both indices differ from each other, in particular when considering recent trends. The Index4 is characterized by a steep decline from the late 1960's on with a relatively weak tendency to recover from 2000 onward. The LL index shows significant variability from 1975 to 1995. Further, the LL index is able to depict the recent upward trend in the stock also visible in YFT stock assessments.

Environmental variables

Disadvantages of using global climate indices which represent 'packages of weather' rather than local conditions, are all related to the fact that another level of problems are added to the ecology–climate interface, namely the link between global climate indices and local climate (Stenseth *et al.*, 2003). Therefore we separate between climate indices and local SST and wind data. Climate indices comprise SST based (TNA, TSA, NTA) and indices including large scale atmospheric pressure differences (ENSO, NAO, PDO).

All time series were resolved to monthly values except for North Atlantic Oscillation and Pacific Decadal Oscillation, for which annual and lag1 and lag2 values were applied. Climate indices and regionalized sea surface temperature data (SST) and wind data (u (zonal), v (meridional) and total wind speed) were obtained from the NOAA-ESRL Physical Sciences Division, Boulder Colorado from their Web site at http://www.esrl.noaa.gov/psd/. Local SST was available from 1981 onward.

The North Tropical Atlantic Index (NTA) is a time series of SST anomalies averaged over 60W to 20W, 6N to 18N and 20W to 10W, 6N to 10N. Anomalies were smoothed by a three months running mean procedure.

The Tropical North Atlantic Index (TNA) is an anomaly of the average of the monthly SST from 5.5N to 23.5N and 15W to 57.5W. The Tropical South Atlantic Index (TSA) was also included in the analysis, but did not prove to be informative.

The El Niño Southern Oscillation (ENSO) affects weather and climate variability worldwide (Stenseth *et al.*, 2003). The index comprises SST anomalies (El Nino) and atmospheric pressure differences (Southern Oscillation).

The North Atlantic Oscillation (NAO) represents the dominant climate pattern in the North Atlantic region (Stenseth *et al.*, 2003). High NAO in the subtropical Atlantic leads to increased deep convection, while in the eastern subtropics O2 fluxes also increase due to the strengthening of the Azores high pressure area, which leads to intensified cooling by

enhanced trade winds (Friedrich *et al.*, 2006), resulting in a negative correlation to SST (Ruiz-Barradas *et al.*, 2000). However, the NAO has no direct link to the equatorial Atlantic (Ruiz-Barradas *et al.*, 2000), but at negative phases trade winds should weaken and thus enhance warming in the eastern tropical Atlantic from 10 – 20 °N (Fromentin, 2002). The index is calculated for the months D-J-F.

The Pacific Decadal Oscillation (PDO) has significant effects on western Atlantic ecosystems (Gherardi *et al.*, 2010). During warm PDO phases, Atlantic SST anomalies in the northern tropical zone are linked to ENSO variability, so that PDO is seen to modify ENSO effects in the Atlantic. Other authors have suggested that PDO and AMO belong to the same atmospheric oscillation pattern (d'Orgeville and Peltier, 2007). Index is calculated for months O-N-D-J-F-M.

Behaviour of fishermen and fish

Local CPUE: Random versus perfect fishermen

The local area considered was 10-20°N latitude and 10-30°W longitude to represent the catching opportunities in the Cape Verde region. Longline data are reported by 1°-squares, and we did not stratify in this small area. Longline CPUE were acquired from the ICCAT "t2ce" database. Two different bases for CPUE were applied for gear type "LL", i.e. long-lining, either CPUE by number caught (CPUE.nr) or by catch weight (CPUE.kg). CPUE by numbers were calculated from 1965 to present. Effort is expressed in terms of number of hooks, although other effort parameters such as gear soak time could be more informative but are not available in the data base (Watson and Kerstetter, 2006). Data for CPUE by weight are only available since 1995.

Both raw and fitted local CPUE were calculated. The raw index is the annual catch divided by the annual effort at local level, assuming that the fisheries targets YFT perfectly and thus has high efficiency. This interpretation is augmented by the absence of zero records in the data base, as normally observations below the economic threshold are underrepresented in fisheries dependent data. Mangel and Clark (1986) point out that detection success is dependent on search rate, and with the high technological standards of the fisheries this can be assumed to be valid. In turn, the fitted index assumes that reported catch records are random samples of the stock. For the fitted model changes in seasonal sampling effort between and within years as well as fleet effects were considered, assuming log-normal distribution of errors (Maunder and Punt, 2004), performed as generalized additive mixed model with fleet and years as fixed effects:

$$\ln(CPUE_l+1) \sim year_i + f(month_k) + fleet_j + \varepsilon_i \qquad \text{Eq. 4}$$

Autocorrelation between residuals was significantly reduced by accounting for autocorrelation between months (Wood, 2017).

Accounting for fish distribution: Type I/II versus type III concentration profiles

The concept of concentration profiles (Clark, 1982) can be applied to distinguish between two basic types of CPUE distributions with regards to area and fish stock based on the partial interchangeability of stock units and spatial units (Hilborn and Walters, 1992). In Type II concentration profiles, CPUE is uniformly distributed in relation to area without any preference to environmental factors (Fig. 1 A). Clark (1982) describes this as distribution along a food gradient, and empty habitat due to harvested fish is immediately replenished from the surrounding stock. This is in line with the Ideal Free Distribution hypothesis where all specimens experience the same fitness, and often applies to ground fish assemblages. Cumulative abundance can be approximated by a power function. In Type III profiles (Fig. 1 B), a middle level CPUE is dominating in terms of spatial coverage. Cumulative abundance can be expressed as sigmoidal curve. It is evident, that for type II profiles no specific weights should be assigned to CPUE values in the modelling, while for type III profile modelling area or catch-specific weighting is optimal to represent the distribution.

The remaining type I and IV profiles can be derived from type III profiles. Type I profiles, where spatial coverage of locations with increasing CPUE decreases constantly, can be interpreted as sampling type III where the middle level is lower than the economic threshold (X_2 in Fig. 1 B), hence there is a uniform decrease in CPUE with abundance. Type IV, the constant concentration profile, can be derived from type III if all fish aggregate into the middle CPUE level and other CPUEs disappear. This applies to actively schooling fishes or colony aggregating mammals or birds, and these populations often show hyper-stability, i.e. while the total stock decreases, local CPUE remains constant. In turn, hyper-depletion occurs if local CPUE decreases more rapidly than abundance.

Tuna often aggregate in schools depending on environmental 'attractors', debris, dolphin schools, floating devices etc., and 'advective' movements are described for aggregations moving to feeding and spawning grounds. On the other hand, within a feeding ground or favourable habitat, diffusive movements are known (Fonteneau and Soubrier, 1996) indicating a tendency for type III and IV models. Skipjack tuna and YFT distribution have been shown to follow type III concentration profiles, with strong declines in CPUE in the beginning of the fisheries and some stabilisation at middle level, all together an indication of hyper-depletion (Hilborn and Walters, 1992).

Consequences in terms of hyperdepletion and hyperstability of fishing regimes

With regards to fishermen behaviour, we can discern between 4 different combinations of fishermen's behaviour and fish distribution in terms of raw and standardized CPUE and applying catch as model weights or not (Fig. 1, C-F). Perfect fishermen tend to fish the best spot first (Clark, 1982; Hilborn and Walters, 1992), so that CPUE drops rapidly in type III profiles while relatively little of the stock is fished (Fig. 1 F). Reaching middle level CPUE, a considerable part of the stock is fished while CPUE remains stable, in fact, the stock curve in Fig. 1 F is the inverse of Fig. 1 B. With only little of the stock remaining, CPUE decreases again, but as mentioned earlier, this is seldom represented in fisheries dependent data since fisheries stops at some economic threshold X_1. In terms of type II

profiles, fishermen would fish the high concentration spots maintaining high CPUE while decreasing stock abundance rapidly (Fig. 1E). In turn, for random fishermen CPUE will likely decrease almost linearly with stock (Fig. 1 C,D).

Model selection and interpretation

The workflow for model selection consists of an (1) initial multiple linear regression model based on best correlations, selecting 15 parameters for CPUE.nr or 25 for CPUE.kg due to differing time series lengths from a suite of 114 environmental variables. Linear models are characterized by their F-statistic and their goodness-of-fit in terms of adjusted r^2, which takes into account an adjustment in relation to the number of parameters in a model. (2) The stepAIC() function in R was applied as first reduction step yielding a model H_{AIC}. It selects a model from a suite of alternative models, and provides the most parsimonious solution given the data available (Burnham *et al.*, 2011), but may contain insignificant and inter-correlated parameters. Therefore, this model is (3) further evaluated for its significant terms yielding a model H_1. Parameters are evaluated with ANOVA type III and the variance-inflation-factor function (VIF), both of the R car package (Fox and Weisberg, 2011), and are removed one-by-one starting with the most insignificant p-value/highest VIF until all parameter estimates were significant with at least $p<0.1$ and VIF < 3. ANOVA type III analyses the model structure with the effect of each parameter on the dependent variable after all other parameters have been partialled out, whereas VIF analyses structure within the suite of independent parameters identifying collinearity. VIF is defined as $1/(1-R_j)$, where R_j is the proportion of variance explained by the multiple regression of parameter j as dependent against all other parameters as independent variables. A VIF threshold of 3 is recommended (Zuur *et al.*, 2010), above which collinearity has a very strong effect on uncertainty in parameter estimates. This threshold is empirical, and including parameters with higher VIF may be advisable in some cases (O'Brien, 2007), and this will be discussed with regards to error structure . H_1 model parameters from the linear models are evaluated across models by means of their standardized or beta coefficients indicating their total contribution to the regression model comparable to partial correlations (Ray-Mukherjee *et al.*, 2014). Beta coefficients were calculated with the lm.beta package in R (R Development Core Team, 2008) and were averaged with parameters not contained in a model set to zero. (4) A generalized additive model (GAM) is applied to the model parameters defined under H_1. The smoothing function in GAM for each parameter was fixed to order 3. The application of a linear model allows a more straightforward interpretation of relationships in terms of correlation, whereas the interpretation of parameters could be difficult for GAMs as standalone tool. (5) Selection by means of Bayesian Model Averaging (BMA) is applied to compare with parameter selection in the H_1 model. BMA is applicable in cases with complex parameter structure and over-parameterization (Reichert and Omlin, 1997). BMA applies no weights in the selection of parameters, therefore model structure is equivalent to type II models. Uniform priors were applied, and intercepts were not estimated. BMA estimates models for all possible combinations of parameters and then constructs a weighted average based on model likelihoods. Statistics include posterior inclusion probability (PIP) and estimated number of parameters in the model as provided

by the bms() function (Feldkircher and Zeugner, 2009). Parameter coefficients were obtained as averages from all model runs including models were the parameters were not contained in which case the coefficients were zero. Precision is estimated as the probability of having an either positive or negative sign, following the p-notation with +, ++, +++ equivalent to 0.95, 0.99, and 0.999 probability of being greater or less than 0.

Results

The LLIndex (Fig. 2) shows a considerable decline in stock size since 1967. Stock size varied between 1970 and 1992, with small peaks in 1974, 1979 and 1990, but after 1992 reached a steady low phase until 2010. Of the two stock indices used, the LLindex had higher correlations with both local CPUE indices and was therefore used for further calculations (Table 2). The representation of stock trend is different between both indices LLindex and Index4, evident by the negative correlation between raw CPUE.kg and Index4, and LLindex indicates an upward trend for recent years, consistent with assessment results (Anonymous, 2016). Of the two local CPUE indices, only raw CPUE.kg is reflecting this upward trend after the year 2000 (Fig. 2), whereas raw CPUE.nr shows a negative trend since 2003 (Fig.3).

CPUE models were evaluated in 2*2*2*2 categories, i.e. CPUE by weight or by number, standardised vs. raw CPUE estimates, type II *vs*. type III models, and with regards to the relationship to Ns, i.e. Ns versus log(Ns). With regards to Ns specifications, changes in Goodness-of-fit (GOF) were equivocal for standardised CPUE and raw CPUE, but on average type III models performed better: For type II models GOF increased from raw to standardised CPUE (0.2 to 0.25 for CPUE.nr; 0.31 to 0.57 for CPUE.kg), whereas for type III models GOF changed equivocal (0.28 to 0.38 for CPUE.nr; 0.59 to 0.45 for CPUE.kg). However, in the case of standardised CPUE.kg negative coefficients were obtained for LL stock index in both type II and III models.

For the best models in terms of GOF, applying log(Ns) instead of Ns according to equations 2a,b increased GOF moderately by 0.04-0.05 (Table 3). Besides increasing GOF statistics, H1 error structure improved in both cases, although heteroscedasticity indicates that H1 model formulation likely left out important parameters (Fig. 4)

The number of estimated model parameters was higher in the BMA models (6-7 parameters) than in the H_1 models (3-4 parameters incl. intercept).

<u>CPUE by weight</u>

CPUE by weight (CPUE.kg) was analysed for years > 1994, and SST was included in the model evaluation process. CPUE.kg resembles the trend of LLindex in terms of an increase after 2005, a drop in 2010 and a subsequent increase since then, however with a low value in 2013 when LLindex in turn reached a high value. The maximum value for CPUE.kg in 2014 is also reached in the HAIC model, but not in the H1 and GAM models (Fig. 1). Besides this, the overall interpretation of CPUE.kg trend is not different between H_{AIC} and H_1 models.

BMA and H_1 models indicated both a negative relationship to TNA in March (TNAmar), and positive wind effects for the u-components (zonal winds, Usep and Uoct), except for the model for standardised Type III CPUE.kg with a lacking wind effect. The positive relationship for u-wind means a weakening of the predominantly easterly winds. The H_1 model identified the September u-component in both Type II models with $p<0.1$ and the October u-component in the raw Type III model with $p<0.05$, whereas BMA indicated weakening in October and in the early summer period May-July, both for raw and standardised CPUE.kg. However, linear models for standardised CPUE by weight performed weakly with regards to the parameterization of the stock LLindex, which was negative. Thus, highest congruency between BMA and H_1 was reached between the Type III model for raw CPUE.kg and the BMA models, encompassing LLindex, Uoct and TNAmar. For graphical interpretation, combining Usep and Uoct and averaging the beta coefficients shows a consistent interpretation of TNAmar and Usep/Uoct in all 4 models, whereas results for LLindex are equivocal (Fig. 5).

CPUE by numbers

The length of the CPUE.nr time series was 50 years, and therefore the shorter SST time series was excluded from this analysis. CPUE.nr reached its highest value in 1979, consistent with the smaller peak in the LLindex, but a smaller peak in CPUE.nr only represents the high stock abundance before 1970. H_{AIC} and H_1 overestimate CPUE.nr before 1970, and underestimate the 1979 peak and the increase 2001-2004 (Fig. 3).

Overall goodness-of-fit was smaller than for CPUE.kg models. All terms in the H_1 type II models were contained in their BMA congeners, encompassing Umay, LLindex for raw CPUE.nr and Umay, LLindex and lag2NAO for standardised CPUE.nr. Type III models contained wind variables Uapr, SPEEDmay and Vsep. The results for Vsep are opposite to the Usep/Uoct results for CPUE.kg. The GAM function for Vsep was zero in the standardized Type III model, when H_1 indicated it was significantly negative NAO was negative in BMA and GAM models, but did not prove to be significant in any H_1 model. The coefficient for LLindex was positive in all cases. The Type III models both showed no congruency with BMA results. The figure of beta coefficients indicates a consistent positive effect of LLindex and a negative effect of Umay/Uapr combined, but weak effects for Lag2NAO and Vsep (Fig. 6).

Discussion

Understanding of model structure

A suite of 114 environmental parameters was introduced so that due to overparameterization a subset had to be selected for analysis based on correlations. Further selection was carried out applying the AIC criterion, the variance inflation factor and significant F-tests. H_{AIC} and H_1 models differed only little (Fig. 1 and Fig. 3), and we consider the H_1 models indicative of the main and significant processes driving local CPUE. These reduction steps are consistent with the prevailing philosophy in modelling

to create simple models, one of the 4 truths in model setup (Crawley, 2002). The other truths state that all models are wrong, some models are better than others and that a correct model can never be known with certainty. Thus, in an exploratory way we performed different modelling methodologies (ordinary least squares vs. BMA) and parametric coefficients as well as non-parametric smoothing to analyse the functional terms (linear *vs*. GAM) and investigated the consistency of results for contrasting hypothesis (II *vs*. type III, perfect vs. random, etc.). Consistency was indicated by means of variable importance plots with standardized coefficients. For CPUE.kg, consistency was found for TNAmar and u-wind components, but the models for standardized CPUE.kg performed less well with respect to negative coefficients for LLindex, indicating that local catch rates should increase with sinking stock size. This is inconsistent with the knowledge of the stock with a wide distribution across the Atlantic warm water sphere (Lan *et al.*, 2011; Arrizabalaga *et al.*, 2015) and no signs of change in spatial patterns (Worm and Tittensor, 2011). For CPUE.nr, Type II models were consistent with their BMA congeners with Umay and LLindex as common parameters, accompanied by lag2NAO in the case of the standardized Type II model.

From the 48 local parameters considered, only 1-2 remained as significant parameters in the H_1 models, although evidently all local variables (SST, u-wind, v-wind, wind speed) must have had an effect on local catch rates, given that they affect the habitat of the shallow dwelling YFT directly (see Arrizabalaga *et al.*, 2015). However, in most cases the application of a VIF threshold of 3 prevented the use of two or more strongly correlated factors, and we see that in the H_1 models closely related parameters may substitute each other, *i.e*. Uoct/Usep for CPUE.kg (Fig. 2) and Umay/Uapr for CPUE.nr (Fig. 4). Thus, the strict application of VIF thresholds constrains the models as evidenced in the H_{AIC} with more functional terms , in that "Simply dropping X_j because it is highly correlated with the X_i or using step-wise regression to select variables (typically the selected variables are not “too highly correlated” with each other) leads to a model that is not theoretically well motivated" (O’Brien, 2007).

Understanding of local stock abundance

4 different CPUE indices with 2 types of models were applied to account for uncertainty in the understanding of local abundance. The application of CPUE.nr or CPUE.kg was dependent on data availability. The rationale for applying raw and standardized annual means was (i) that for raw CPUE we assume that catch rate in those records with catches is representative of what is present, (ii) whereas for standardized CPUE we refilled the month-year table of records based on the theorems of stratified sampling (Walters, 2003). In the case of spatial sampling on a concentrated stock, Walters (2003) pointed out that the raw approach would be confounded by missing entries if they had not been replaced by zero's. In our study, for CPUE.nr no zero entries were indicated and for CPUE.kg, 3 zero entries were found (1995:2, 1997:1), which were not replaced with zero, but by the mean. It is not likely that this affected the analysis, because CPUE.kg was low in that period

(Fig.1). In published studies both raw CPUE (Lan *et al.*, 2011) and standardized CPUE with year and month factors (split into 15 days) (Maury *et al.*, 2001) were applied.

Taking into account the behaviour of the fleet (aggregating, information exchange, application of technical devices to detect schools) and the behaviour of the fishes (schooling, aggregation along fronts (Doray *et al.*, 2009)), the raw CPUE Type III models appear appropriate, consistent with the analysis of Maury *et al.* (2001) that effort is a significant parameter in longline CPUE. Nevertheless, CPUE models differ between studies. We separated the model into three components, i.e. local CPUE, stock size and environmental factors with local CPUE standardized with fleet, year and month effect. Maury et al. (2001) applied a slightly different setup analysing local CPUE in each rectangle as a function of year and month effect to 'account for biomass fluctuations', plus environmental factors, and Lan *et al*. (2011) and Doray *et al*. (2009) applied principal components analysis to the CPUE-environment matrix not specifically accounting for stock effects. In turn, the analysis of Doray et al. (2009) and our study focussed on a regionalised or mesoscale approach (~ 500 km), whereas Lan *et al*. (2011) and Maury et al. (2001) analysed the entire range of distribution.

Both YFT CPUE by weight (Maury *et al.*, 2001; Doray *et al.*, 2009)and by numbers caught (Lan *et al.*, 2011) have been applied in the literature. In this study, the congruency between CPUE.kg Type II and Type III results and the easy interpretation of the resp. beta coefficients (Fig. 2) indicates that CPUE.kg models enable a better understanding of CPUE dynamics. In particular, CPUE.kg is able to reflect the increase in YFT stock after 2000, which was also seen in Taiwanese long-line data (Lan *et al.*, 2011).

Interpretation of environmental factors

Present studies on XFT habitat acquire environmental parameters from a mix of sources, *i.e.* coupled hydrodynamic and biogeochemical models (Maury *et al.*, 2001; Lan *et al.*, 2011; Arrizabalaga *et al.*, 2015), satellite data and climate indices (Doray *et al.*, 2009; Lan *et al.*, 2011) and additional in situ measurements (CTD casts and hydroacoustics, Doray *et al.*, 2009). We acquired long-term reanalysis data series and climate indices rather than model output.

This limits our analysis with respect to salinity, subsurface temperature and accordingly thermocline depth, important parameters in all three above mentioned studies. In turn, the focus on a certain region allows us to investigate seasonal effects. We can find consistencies with regards to the interpretation of environmental influences. For CPUE.kg, TNAmar (negative) and Usep/Uoct (positive) were identified as H_1 parameters (Fig. 2). This indicates cooling with a subsequent deepening of the mixed layer (MLD) in March and a calming down of zonal winds in autumn. With regards to MLD, explanations either point at direct relationships so that MLD was positively correlated with YFT CPUE and explained more inertia/variance than remaining SST, temperature at 150 m and salinity together (Maury *et al.*, 2001). Indirectly, due to enhanced mixing, more nutrients

would entrain the surface layer supporting primary and enhance secondary production. Doray *et al*. (2009) accordingly showed that YFT biomass was related to the micronekton abundance, partially driven by increased primary production in freshwater influenced areas of the Orinoco plume. However, Bertrand *et al*. (2002) showed that the relationship between YFT CPUE and micronekton density further depends on behavioural aspects, given that generally a positive relationship between prey density and YFT CPUE exists, but as soon as prey is present in high density patches, CPUE declines due to an assumed switch in feeding with a preferential uptake of prey rather than long-line bait. The cooling in spring is further partially indicated in the positive relationship to NAO and intensified Uapr/Umay winds in the CPUE.nr H_1 models, since a positive NAO enhances the trade winds and thus deepens the mixed layer depth (Fromentin, 2002).

Calm autumn winds are linked to the seasonal shift of the ITCZ which moves to about 12-14°N in autumn. The ITCZ moves northward with a rate of 0.38° per 24 yrs (Zagaglia *et al.*, 2004; Colna, 2017). The link to ITCZ position was also indicated for the western tropical Atlantic, where fisheries is enhanced in and south of the ITCZ (Zagaglia *et al.*, 2004).

A series of publications investigates the role of NAO in triggering tuna stocks (Santiago, 1998; Die *et al.*, 2002; Fromentin, 2002; Rubio *et al.*, 2016). Primary effects were expected for recruitment, which would explain the weak negative lag2NAO relationship for CPUE.nr in this study. A lag2 relationship would indicate a calming down of trade winds 2 years before, indicating enhanced warming in surface waters. However, evidence at best is equivocal for a NAO-YFT relationship (see Die *et al.*, 2002; Fromentin, 2002). Rouyer *et al*. (2008) showed that NAO was significant for tuna stocks only north of 20°N in line with the equivocal relationship found here.

Synthesis of prey field dynamics and the analysis of tuna dynamics to qualitatively evaluate the prospect for future fisheries in the tropical eastern central Atlantic

Abstract

The evaluation is based on the analysis of prey length spectra and biomass size spectra on the one side and tuna catch rate dynamics on the other side. The production of tuna is determined by the amount of primary production PP transferred to higher trophic levels TL by PP × TE $^{(TL\ -\ 1)}$, where TE is trophic efficiency. TE is determined by TE=exp((b-0.25)*lg PPMR), where b is the slope of biomass spectrum and PPMR is the size ratio of predators to prey. The analysis of prey dynamics revealed no change in minimum or maximum sizes of the species indicating no change in PPMR. However, significant differences in size structure were indicated in 20 out 28 species. Slopes of normalized biomass size spectra steepened in 2015 for the tropical (-0.88 to -1.4) and subtropical

region (-1.08 to -1.28). The slope for the temperate region was -0.44 in 1966-79. Maximum sizes for all species were smaller in the oxygen minimum region, associated with significant changes in size structure.

Local dynamics of Yellowfin tuna (*Thunnus albacares*, YFT) catch rates covering the area 10-20°N latitude and 10-30°W longitude indicate a positive dependency on cooling in the tropical North Atlantic in springtime and a weakening of autumn winds in September and October. The evaluation shows that negative effects due to changes in TE can be counterbalanced by improved stock management.

Introduction

The link to reconcile results from both fields of PREFACE WP12.1 is to apply principles of ecological production in relation to forage fish and tuna, evaluate bioclimatic effects as evidenced from updated D 12.2 and combine both aspects into a qualitative framework.

Ecosystem theory

Food chain models predict that production P at any trophic level TL, *i.e.* tuna as apex predators, is determined by the amount of primary production PP transferred to higher trophic levels with transfer efficiency TE (Jennings and Blanchard, 2004)

$$P \approx PP \times TE^{(TL-1)} \qquad \text{Eq. 5}$$

This underpins the need for understanding changes in TE in the ecosystem.

TE can be determined from the slope of biomass-size spectra (BSS). In a review on BSS, Menezes dos Santos et al. (2017) stated that BSS are important indicators of biomass distribution, both for fundamental understanding as well as for application in management. Any change in community structure of ecosystems will become evident also in terms of distinct allometric scaling with a subsequent change in BSS as a distribution of community biomass over size classes. BSS generally respond to stress by means of a decrease of the slope, as suggested by most of the studied models, is supported by the data found in their review (Menezes dos Santos *et al.*, 2017). The investigated empirical studies revealed a strong trend for the slope: 40 out of 57 studies reported a decrease with stress. Stress includes inter alia increase in nutrients and increased primary production, but also fishing activities and physical stress such as heat etc. Changes may affect both slope and intercept of BSS. Gascuel et al. (2005) show that a decrease in larger size groups combined with an increase in smaller size groups also results in a steepening of slope. However, the increase in smaller size classes is indicative of reduced predatory pressure due to a decrease in abundance of larger predators and thus indicates a top-down effect and meso-predator release as was shown for changes in BSS after intense fishing for tuna and billfishes (Baum and Worm, 2009).

The slope b of BSS kann be expressed as (Jennings and Blanchard, 2004)

$$b \approx \log_{10}TE/\log_{10}PPMR+0.25 \qquad \text{Eq. 6a}$$

$$TE=10^{(b-0.25)*\log_{10} PPMR)} \quad \text{Eq. 6b}$$

where PPMR is the biomass ratio between predators and prey.

Evidence form forage fish dynamics

Normalized BBS slopes increased from 1966-72 to 2015 in the area steepened from -0.88 to -1.4 in the tropical zone and from -1.08 to – 1.28 in the subtropical zone (Fig. 7)(Fock and Czudaj, n.d.). BSS included size groups from 2^0 to 2^7g. In the tropics, size groups 2^0 and 2^1 g increased in abundance while larger size groups decreased in biomass indicative of a top-down effect. The steepening of the slope in both areas indicates reduced TE probably in line with an increase in overall production in the areas, which was shown to influence regional OMZ dynamics (Hahn *et al.*, 2017).

Evidencen from Yellowfin tuna bioclimatic modelling

Two basic patterns were evident in the tuna bioclimatic modelling, i.e. a dependency on autumn winds and second a relationship to spring cooling in the upper ocean layer. The wind effect was very clear for meridional winds in September and October, indicating a calming down in all 4 model specification for YFT CPUE.kg, and an increase in zonal winds in September in 1 of the 4 models for YFT CPUE.nr. Zagaglia *et al.* (2004) found the same relationship between autumn wind and YFT catches for Brazil, and show that this is related to the northerly seasonal shift of the Intertropical Convergence Zone (ITCZ).

The second consistent pattern is the cooling in spring evidenced by a negative NTA anomaly in March and increased meridional winds in April and May. As discussed for effects of NAO, increased wind leads to deeper mixed –layer depths, and the entrainment of deeper water decreases SST. Altogether, this effect is assumed to reflect increases in primary productivity and enhanced production of plankton and forage fishes. Also, for the zone near the African coast, increased offshore transport of upwelled and plankton rich waters may be augmented from increased winds. NAO increased from the

A third patterns appears for the influence of the total stock on regional CPUEs. These are significant in the long-term for CPUE.nr, and for CPUE.kg, although negative effect with regards to standardized CPUE.kg and positive effects with regards to raw CPUE.kg appeared, model performance was increased using a $\log(N_s)$ relationship in line with the 'pipeline' model (Fig. 4) (Fonteneau and Soubrier, 1996) indicative of direct link between total stock and local CPUE. Recent assessments (Anonymous, 2016) indicate that stock biomass is increasing and approaching the MSY-level for maximum sustainable yield.

Reconciling evidence

The human impact on the regional tuna stock is evidenced by means of the significant effect of stock index in all CPUE.nr models and the improvement of model performance in

CPUE.kg models based on the 'pipeline' effect (Fig. 4). The former applies to the longer time series, whereas for the shorter time series on CPUE.kg when the stock was on low levels, the stock effect was not as clear in terms parameter significance except for the 'pipeline' effect. The decline of stock size due to overfishing had a significant long-term effect, whereas at already low levels, stock size's importance was equivocal (CPUE.kg models). This highlights the important role of MSY-orientated management for maintaining regional catch opportunities.

The autumn wind effect and the spring effects comprising wind and SST effects pointed at seasonal cooling, appear both in long- and the short-term analysis. However, in the long-term the spring effect prevails, while in the short-term both effects appear equally important.

Assessing future tendencies of autumn and spring effects, seasonal ITCZ movements appear to be stable with a little tendency to move further north in autumn. However, this tendency was only 0.4° in 3 decades (Colna, 2017). The overall positive trend for NAO also appears stable, and the highest value since 1950 was recorded in 2015. High NAO is associated with increased subtropical deep convection and increased trade winds in the eastern subtropics due to the strengthening of the Azores high pressure area, which leads to intensified cooling (Fromentin, 2002; Friedrich *et al.*, 2006).

The abundance of forage fish did not decrease, but BSS slopes increased in the tropics and subtropics. This could point at increased community stress due to changes in primary productivity which would appear as effect of enhanced wind mixing. On the other hand, analysis of remote sensing data 1998-2014 (Demarcq and Benazzouz, 2015) reveals a negative trend in the area except for waters off Guinea and northern Morocco. This in turn could indicate that the meso-predator release effect indicated by the shift in BSS in advantage of smaller specimens could be more important. In fact, Fig. 3 shows that the change in apex predators such as YFT was significant from the 1960's to present.

References

Anonymous. 2011. Report of the 2011 ICCAT Yellowfin Tuna stock assessment session. 50-51 pp.

Anonymous. 2016. Report of the 2016 ICCAT yellowfin tuna stock assessment session. Collect. Vol. Sci. Pap. ICCAT, 68: 655–817.

Arrizabalaga, H., Dufour, F., Kell, L., Merino, G., Ibaibarriaga, L., Chust, G., Irigoien, X., *et al.* 2015. Global habitat preferences of commercially valuable tuna. Deep Sea Research II, 113: 102–112.

Baum, J. K., and Worm, B. 2009. Cascading top-down effects of changing oceanic predator abundances. Journal of Animal Ecology, 78: 699–714.

Bertrand, A., Josse, E., Bach, P., Gros, P., and Dagorn, L. 2002. Hydrological and trophic characteristics of tuna habitat: consequences on tuna distribution and longline catchability. Canadian Journal of Fisheries and Aquatic Sciences, 59: 1002–1013. http://www.nrcresearchpress.com/doi/abs/10.1139/f02-073.

Burnham, K. P., and Anderson, D. R. 2004. Multimodal Inference - Understanding AIC and BIC in Model Selection. Sociological Methods & Research, 33: 261–304.

Burnham, K. P., Anderson, D. R., and Huyvaert, K. P. 2011. AIC model selection and multimodel inference in behavioral ecology: Some background, observations, and comparisons. Behavioral Ecology and Sociobiology, 65: 23–35.

Clark, C. W. 1982. Concentration Profiles and the Production and Management of Marine Fisheries.

Colna, K. E. 2017. Latitudinal Position and Trend of the Intertropical Convergence Zone (ITCZ) and its Relationship with Upwelling in the Southern Caribbean Sea and Global Climate Indices. 99 pp.

Crawley, M. J. 2002. Statistical Computing. 761 pp.

d'Orgeville, M., and Peltier, W. R. 2007. On the Pacific Decadal Oscillation and the Atlantic Multidecadal Oscillation: Might they be related? Geophysical Research Letters, 34: 3–7.

Demarcq, H., and Benazzouz, A. 2015. Trends in Phytoplankton and Primary Productivity off Northwest Africa. Paris. 331-341 pp.

Die, D., Kell, L., and Pallares, P. 2002. Time trends in abundance and catchability of yellowfin tuna and their relationship to the North Atlantic Oscillation Index. Collective volume of scientific papers International Commission for the Conservation of Atlantic Tunas/Recueil de documents scientifiques Commission internationale pour la Conservation des Thonides de l'Atlantique/Coleccion de documentos cientificos, Sci. Pap.: 1049–1063.

Doray, M., Petitgas, P., Nelson, L., Mahevas, S., Josse, E., and Reynal, L. 2009. The influence of the environment on the variability of monthly tuna biomass around a moored, fish-aggregating device. ICES Journal of Marine Science, 66: 1410–1416.

Feldkircher, M., and Zeugner, S. 2009. Benchmark Priors Revisited: On Adaptive Shrinkage and the Supermodel Effect in Bayesian Model Averaging. IMF Working Paper 09-202.

Fock, H. O., and Czudaj, S. (n.d.). Size structure changes and biomass size spectra of

mesopelagic fishes along a transect from the Equator to the Bay of Biscay collected in 1966-1979 and 2015. in revision.

Fonteneau, A., and Soubrier, P. P. 1996. Interactions between tuna fisheries: A global review with specific examples from the Atlantic Ocean. *In* Proceedings of the second FAO Expert Consultation Interactions of Pacific Tuna Fisheries. Shimizu, Japan, 23-31 January 1995, p. 612. Ed. by R. S. Shomura, J. Majkowski, and R. F. Harman. Fisheries Technical Paper. No. 365. Rome, FAO, Rome.

Fox, J., and Weisberg, S. 2011. An R Companion to Applied Regression. Sage.

Friedrich, T., Oschlies, A., and Eden, C. 2006. Role of wind stress and heat fluxes in interannual-to-decadal variability of air-sea CO2 and O2 fluxes in the North Atlantic. Geophysical Research Letters, 33: 2–6.

Fromentin, J.-M. 2002. Is the recruitment a key biological process in the hypothetical NAO-Atlantic tunas relationships? Collective Volume of Scientific Papers ICCAT, 54: 1008–1016.

Gascuel, D., Bozec, Y. M., Chassot, E., Colomb, A., and Laurans, M. 2005. The trophic spectrum: Theory and application as an ecosystem indicator. ICES Journal of Marine Science, 62: 443–452.

Gherardi, D. F. M., Paes, E. T., Soares, H. C., Pezzi, L. P., and Kayano, M. T. 2010. Differences between spatial patterns of climate variability and large marine ecosystems in the western South Atlantic. Pan-American Journal of Aquatic Sciences, 5: 310–319.

Hahn, J., Brandt, P., Schmidtko, S., and Krahmann, G. 2017. Decadal oxygen change in the eastern tropical North Atlantic. Ocean Science, 13: 551–576.

Hilborn, R., and Walters, C. J. 1992. Quantitative Fisheries Stock Assessment. Kluwer Academic Publishers, Boston. 570 pp.

Jennings, S., and Blanchard, J. L. 2004. Fish abundance with no fishing: predictions based on macroecelogical theory. Journal of Animal Ecology, 73: 632–642.

Lan, K.-W., Lee, M.-A., Lu, H.-J., Shieh, W.-J., Lin, W.-K., and Kao, S.-C. 2011. Ocean variations associated with fishing conditions for yellowfin tuna (Thunnus albacares) in the equatorial Atlantic Ocean. ICES Journal of Marine Science: Journal du Conseil, 68: 1063–1071. http://icesjms.oxfordjournals.org/content/68/6/1063.abstract.

Lan, K. W., Evans, K., and Lee, M. A. 2013. Effects of climate variability on the distribution and fishing conditions of yellowfin tuna (*Thunnus albacares*) in the western Indian Ocean. Climatic Change, 119: 63–77.

Lee, Y. C., Nishida, T., and Mohri, M. 2005. Separation of the Taiwanese regular and deep tuna longliners in the Indian Ocean using bigeye tuna catch ratios. Fisheries Science, 71: 1256–1263.

Lopez, J., Moreno, G., Lennert-Cody, C., Maunder, M., Sancristobal, I., Caballero, A., and Dagorn, L. 2017. Environmental preferences of tuna and non-tuna species associated with drifting fish aggregating devices (DFADs) in the Atlantic Ocean, ascertained through fishers' echo-sounder buoys. Deep-Sea Research Part II: Topical Studies in Oceanography, 140: 127–138. Elsevier Ltd. http://dx.doi.org/10.1016/j.dsr2.2017.02.007.

Mangel, M., and Clark, C. 1986. Search Theory in Natural Resource Modeling. Natural Resource Modeling, 1: 3–54.

Maunder, M. N., and Punt, A. E. 2004. Standardizing catch and effort data: A review of recent approaches. Fisheries Research, 70: 141–159.

Maunder, M. N., Sibert, J. R., Fonteneau, A., Hampton, J., Kleiber, P., and Harley, S. J. 2006. Interpreting catch per unit effort data to assess the status of individual stocks and communities. ICES Journal of Marine Science, 63: 1373–1385.

Maury, O., Gascuel, D., Marsac, F., Fonteneau, A., and Rosa, A.-L. De. 2001. Hierarchical interpretation of nonlinear relationships linking yellowfin tuna (<i>Thunnus albacares</i>) distribution to the environment in the Atlantic Ocean. Canadian Journal of Fisheries and Aquatic Sciences, 58: 458–469. http://www.nrc.ca/cgi-bin/cisti/journals/rp/rp2_abst_e?cjfas_f00-261_58_ns_nf_cjfas58-01.

Menezes dos Santos, R., Hilbers, P. J., and Hendriks, J. A. 2017. Evaluation of models capacity to predict size spectra parameters in ecosystems under stress. Ecological Indicators, 79: 114–121. Elsevier. http://dx.doi.org/10.1016/j.ecolind.2017.04.017.

O'Brien, R. M. 2007. A caution regarding rules of thumb for variance inflation factors. Quality and Quantity, 41: 673–690.

R Development Core Team. 2008. R: A language and environment for statistical computing. R Foundation for Statistical Computing, Vienna, Austria. www.R-project.org.

Ray-Mukherjee, J., Nimon, K., Mukherjee, S., Morris, D. W., Slotow, R., and Hamer, M. 2014. Using commonality analysis in multiple regressions: A tool to decompose regression effects in the face of multicollinearity. Methods in Ecology and Evolution, 5: 320–328.

Reichert, P., and Omlin, M. 1997. On the usefulness of overparameterized ecological models. Ecological Modelling, 95: 289–299.

Rouyer, T., Fromentin, J.-M., Menard, F., Cazelles, B., Briand, K., Pianet, R., Planque, B., *et al.* 2008. Complex interplays among population dynamics, environmental forcing, and exploitation in fisheries. Proceedings of the National Academy of Sciences, 105: 5420–5425. http://www.pnas.org/cgi/doi/10.1073/pnas.0709034105.

Rubio, C. J., Macías, D., Camiñas, J. A., Fernández, I. L., and Báez, J. C. 2016. Effects of the North Atlantic Oscillation on Spanish catches of albacore , Thunnus alalunga , and yellowfin tuna , Thunnus albacares , in the North – east Atlantic Ocean. Animal Biodiversity and Conservation, 39: 10–13.

Ruiz-Barradas, A., Carton, J. A., and Nigam, S. 2000. Structure of Interannual-to-Decadal Climate Variability in the Tropical Atlantic Sector. Journal of Climate, 13: 3285–3297. http://journals.ametsoc.org/doi/abs/10.1175/1520-0442(2000)013%3C3285:SOITDC%3E2.0.CO%3B2%5Cnhttp://journals.ametsoc.org/doi/abs/10.1175/1520-0442%282000%29013%3C3285%3ASOITDC%3E2.0.CO%3B2.

Santiago, J. 1998. The North Atlantic oscillation and recruitment of temperate tunas. Collective volume of scientific papers International Commission for the Conservation of Atlantic Tunas/Recueil de documents scientifiques Commission internationale pour la conservation des thonides de l'Atlantique/Coleccion de documentos cientificos, Sci. Pap.: 240–249.

Stenseth, N. C., Ottersen, G., Hurrell, J. W., Mysterud, A., Lima, M., Chan, K.-S., Yoccoz, N. G., *et al.* 2003. Studying climate effects on ecology through the use of climate indices: the North Atlantic Oscillation, El Nino Southern Oscillation and beyond. Proceedings of

the Royal Society B: Biological Sciences, 270: 2087–2096. http://rspb.royalsocietypublishing.org/cgi/doi/10.1098/rspb.2003.2415.

Stobberup, K., Amorim, P., Pires, V., and Monteiro, V. 2005. Assessing the effects of fishing in Cape Verde and Guinea Bissau, northwest Africa. Fisheries Assessment and Management in Data-Limited Situations, 21: 395–417. http://apps.isiknowledge.com/full_record.do?product=WOS&search_mode=GeneralSearch&qid=13&SID=Y1KCGNC8E6mGce1E1Om&page=1&doc=1.

Walters, C. 2003. Folly and fantasy in the analysis of spatial catch rate data. Canadian Journal of Fisheries and Aquatic Science, 60: 1433–1436.

Watson, J., and Kerstetter, D. 2006. Pelagic longline fishing gear: a brief history and review of research efforts to improve selectivity. Marine Technology Society, 40: 5–10. http://www.ingentaconnect.com/content/mts/mtsj/2006/00000040/00000003/art00003.

Wood, S. N. 2017. Generalized Addtive Models. 475 pp.

Worm, B., and Tittensor, D. P. 2011. Range contraction in large pelagic predators. Proc. Nat. Ac. Sc. USA, 108: 11942–11947.

Zagaglia, C. R., Lorenzzetti, J. A., and Stech, J. L. 2004. Remote sensing data and longline catches of yellowfin tuna (Thunnus albacares) in the equatorial Atlantic. Remote Sensing of Environment, 93: 267–281.

Zuur, A. F., Ieno, E. N., and Elphick, C. S. 2010. A protocol for data exploration to avoid common statistical problems. Methods in Ecology and Evolution, 1: 3–14.

Tables and Figures

Table 1:

Outline of model specifications.

Source of uncertainty for local CPUE	Specifications	Formal solution
Relationship to total stock	2 model specifications for 'pipeline' model and dependency on higher values	f(Ns) and f(logNs) (see Eq. 2)
Behaviour of fish stock	2 model specifications for uniformly distributed CPUE and aggregated CPUE	Application of Clark's (1982) type II and type III concentration profiles with differential model weighting
Behaviour of fishermen with regards to $CPUE_l$	2 specifications for 'random' and 'perfect' fishermen	$CPUE_l$ either as raw $CPUE_l$ or as standardised value with regards to fleet, season, and year
Differences in $CPUE_l$ with regards to basis of count	2 specifications for numbers and weight caught	Calculation of $CPUE_l$.nr and $CPUE_l$.kg
Change in target species	Selection of samples with low share of Bigeye tuna	The ratio approach of Lee et al. (Lee *et al.*, 2005; Lan *et al.*, 2011) was applied to define catches targeting YFT. A ratio < 0.6 for the sum of bigeye tuna (BET) over the sum of BET, YFT, albacore and swordfish was used to separate from operations targeting BET.

Table 2:

Correlations between CPUE and stock indices.

Variable	Index4	LLindex
Raw CPUE.nr	0.25	0.32
Raw CPUE.kg	-0.27	0.38
Standardized CPUE.nr	0.32	0.39
Standardized CPUE.kg	0.13	0.20

Table 3: Model performance for CPUE.nr and CPUE.kg models, *i.e*. linear modelling (H_1 , H_{1log}), GAM and Bayesian averaging. H_1 models refer to models with untransformed stock data (N_s), H_{1log} models refers to models with log-transformed stock data (log(N_s)). VIF – Variance inflation factor, PIP – posterior inclusion probability.

Variable	H_1 linear model	Estimate/value	H_1 VIF	H_{1log} model	Estimate/value	H_{1log} VIF	GAM#	Estimate##	Bayesian model	Estimate''/value	PIP
Raw CPUE.kg Type II	Adj r^2	0.31					Adj r^2	0.54	Mean no. regressors	5.1	
	Model F-test, p	0.02									
	Intercept**	-2.2									
	Usep'	1.0	1.13				Usep*	positive			
	TNAmar'	-0.9	1.03				TNAmar**	negative	TNAmar	-0.03	26
	LLindex	0.54	1.09				LLindex	positive	LLindex°°°	0.15	100
									Umay+++	0.20	79
									Ujun+++	0.14	68
									Ujul+++	0.08	47
									Uoct+++	0.02	34
Raw CPUE.kg Type III	Adj r^2	0.59		Adj r^2	0.63		Adj r^2	0.47			
	Intercept	-2.0		Intercept	-1.5						
	Model F-test, p	<0.001		Model F-test	<0.001						
	Uoct*	0.8	2.02	Usep*	0.96	1.8	Uoct**	positive			
	TNAmar'	-0.8	1.23	TNAmar'	-0.74	1.3	TNAmar'	negative			
	LLindex	0.8	1.97	(log)LLindex	0.95	1.8	LLindex	-			
Standardized CPUE.kg Type II	Adj r^2	0.57					Adj r^2	0.95	Mean no. regressors	5.1	
	Model F-test, p	0.001									
	Intercept	0.45									
	TNAmar**	-2.26	1.04				TNAmar**	negative	TNAmar	-0.02	25

	Usep'	1.12	1.12				Usep**	Positive			
	LLindex*	-2.6	1.08				LLindex***	Positive at low values	LLindex°°°	0.15	100
									Umay+++	0.20	79
									Ujun+++	0.13	66
									Ujul+++	0.07	42
									Uoct+++	0.02	40
Standardised CPUE.kg Type III	Adj r^2	0.45					Adj r^2	0.86			
	Intercept	-1.9									
	Model F-test	0.003									
	TNAmar***	-2.09	1.18				TNAmar***	negative			
	LLindex	-0.76	1.18				LLindex**	positive at low values			
Raw CPUE.nr Type II	Adj r^2	0.20					Adj r^2	0.21	Mean no. regressors	6.2	
	Model F-test	p=0.002									
	Intercept***	-7.1									
	Umay*	-0.6	1.005				Umay'	negative	Umay+++	-0.002	69
	LLindex**	0.3	1.005				LLindex**	positive	LLindex°°°	0.0007	100
									NAO+++	-0.0004	44
									TSAfeb+++	-0.0005	30
									Usep+++	-0.0006	30
									Uapr+++	-0.0004	27
									Ujan+	0.0001	25
Raw CPUE.nr Type III	Adj r^2	0.28					Adj r^2	0.22			
	Model F-test	p=0.00032									
	Intercept*	-12.13.0									

	UaprVsep'	-0.241.2	1.2978				Vsep	Negative at low values-			
	SPEEDmay NAO'*	1.030.4	1.334				NAO	-Negative			
	LLindex**	0.447	1.112.23				LLindex**	Positive			
Standardized CPUE.nr Type II	Adj r^2	0.25					Adj r^2	0.29	Mean no. regressors	5.1	
	Model F-test	p=0.001									
	Intercept***	-6.9									
	Lag2NAO*	-0.2	1.26				Lag2NAO*	negative	Lag2NAO+++	-0.0004	52
	Umay'	-0.5	1.01				Umay	negative	Umay+++	-0.002	69
	LLindex*	0.24	1.28				LLindex*	positive	LLindex+++	0.0004	50
									NAO+++	-0.0002	49
									Vjan+++	0.0003	42
									Ujan++	0.0002	34
Standardized CPUE.nr Type III	Adj r^2	0.38		Adj r^2	0.43		Adj r^2	0.15			
	Model F-test	p<0.001		Model F-test	p<0.001						
	Intercept***	-6.7		Intercept***	-6.5						
	Uapr'	-0.4	2.08	Uapr**	-0.43	2.3	Voct	-			
	Vsep**	-0.7	2.3	Vsep*	-0.45	2.1	Vsep	-			
	LLindex**	0.3	1.18	LLindex***	0.58	1.3	LLindex**	positive			

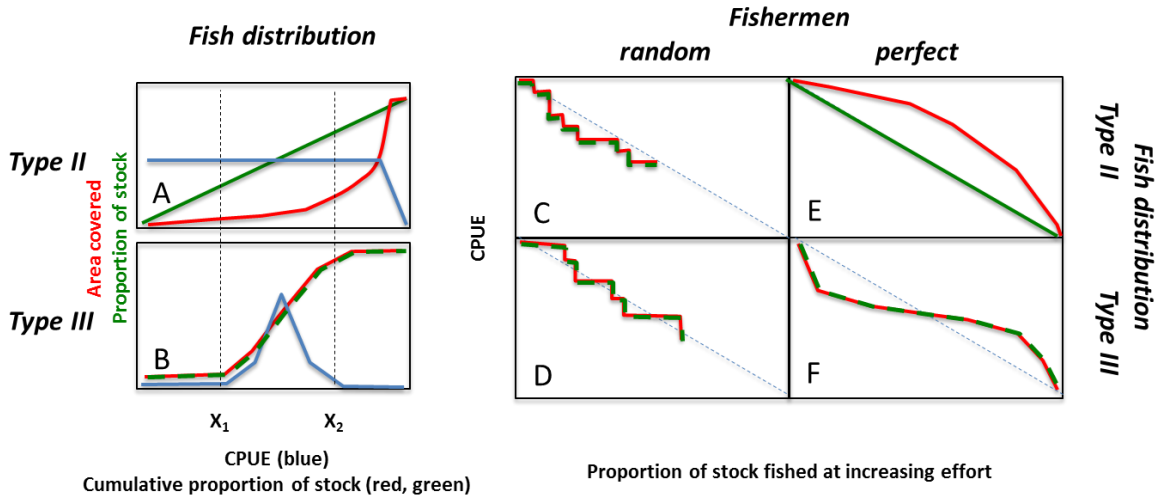

Fig. 1

Clark's (1982) type II and III CPUE concentration profiles with respect to cumulative stock (green) or cumulative area covered (red). (A) CPUE is uniformly distributed across stock or space, so that cumulative abundance is a straight line (green) are curvilinear (red). With perfect fishermen interacting with the stock, the decline in stock abundance is the inverse of the cumulative abundance, so that with regards to area hyperstability will appear (E). With a modal distribution across space or stock, a sigmoidal increase occurs (B), so that in a perfect fisheries in the stage a rapid decrease in CPUE occurs (hyperdepletion), followed by a stage of relative stability (hyperstability) (F).

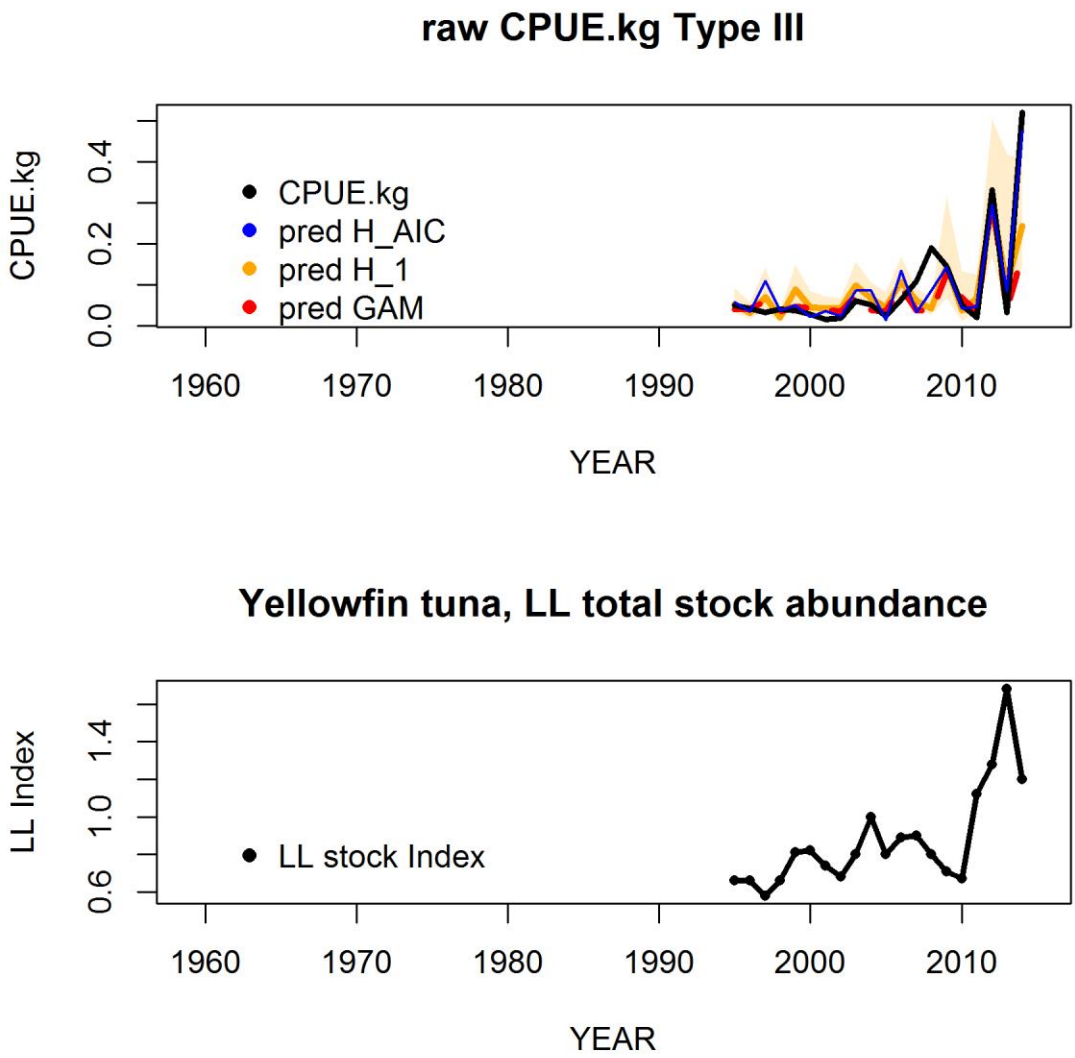

Fig. 2:

Best model for CPUE.kg and corresponding time series of stock index LLindex.

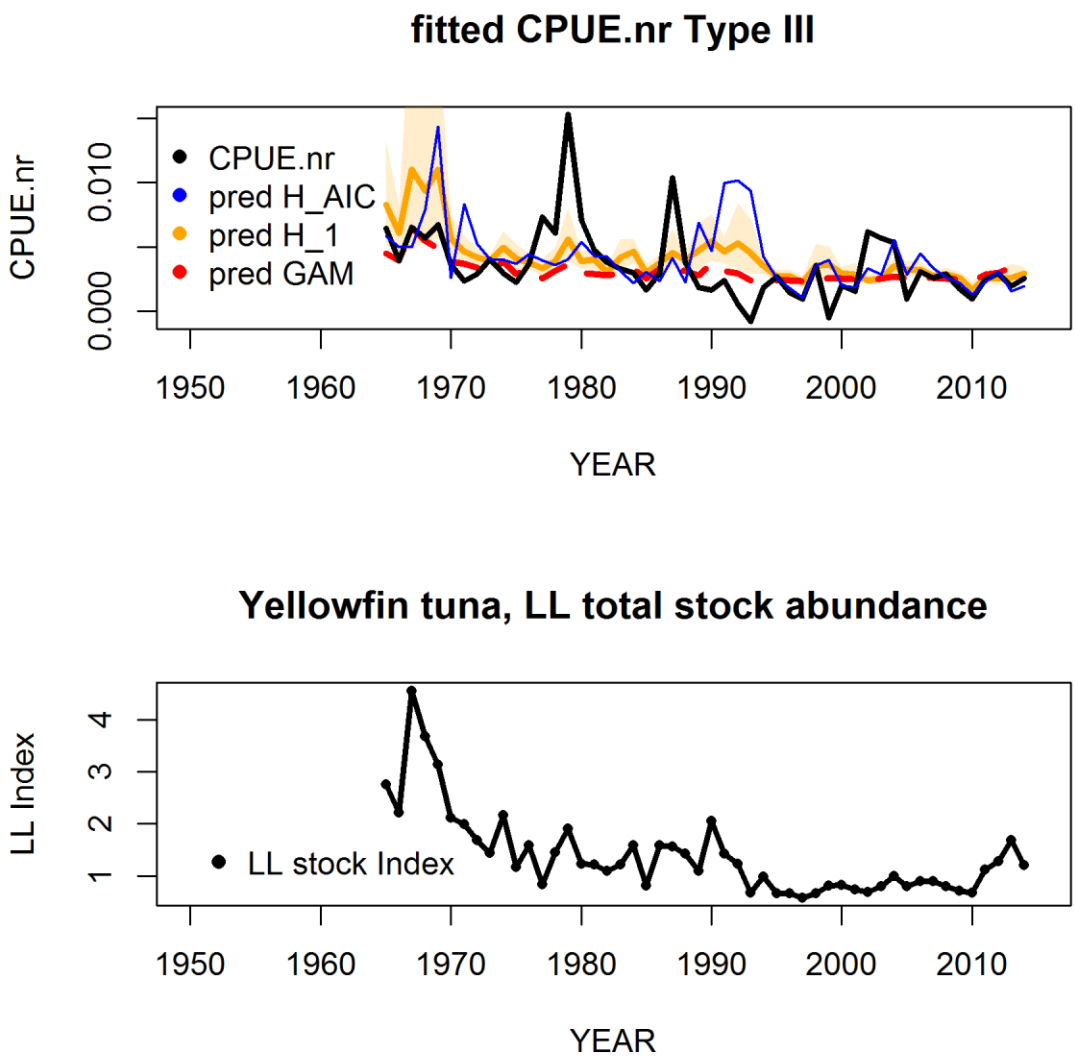

Fig. 3:

Best model for CPUE.nr and corresponding time series of stock index LLindex.

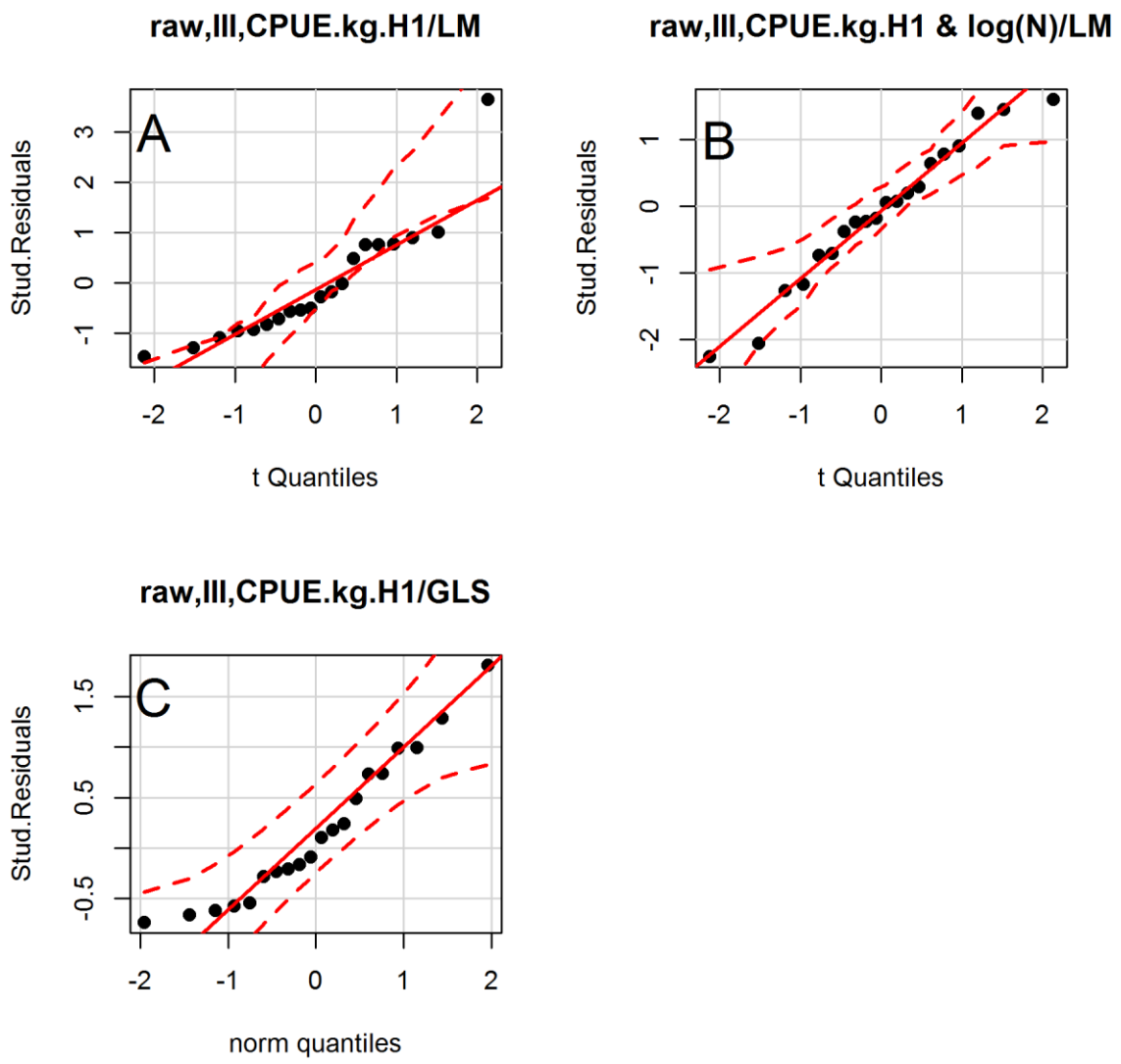

Fig. 4:

Effect of log(N_s) and treatment of error structure with Generalized Least Squares method (GLS) on model performance. Sigmoid error structure in (A) indicates heteroscedasticity and error autocorrelation, which is partly removed in (B) by taking log(Ns) and in (C) by GLS to combat error structure. AIC in (A) 53.7, (B) 51.9 and (C) 55.8, indicating a preference for models with log(N_s). 95% confidence interval for overlap with normal distribution indicated. LM = ordinary least squares modelling. The difference in AIC between (B) and (C) shows that (B) is superior to (C), whereas the difference between (A) and (B) is inferior so that both models have substantial support (see Burnham and Anderson, 2004). With the information of additional GOF parameters and residual plot (B) the model with log(N_s) appears preferable.

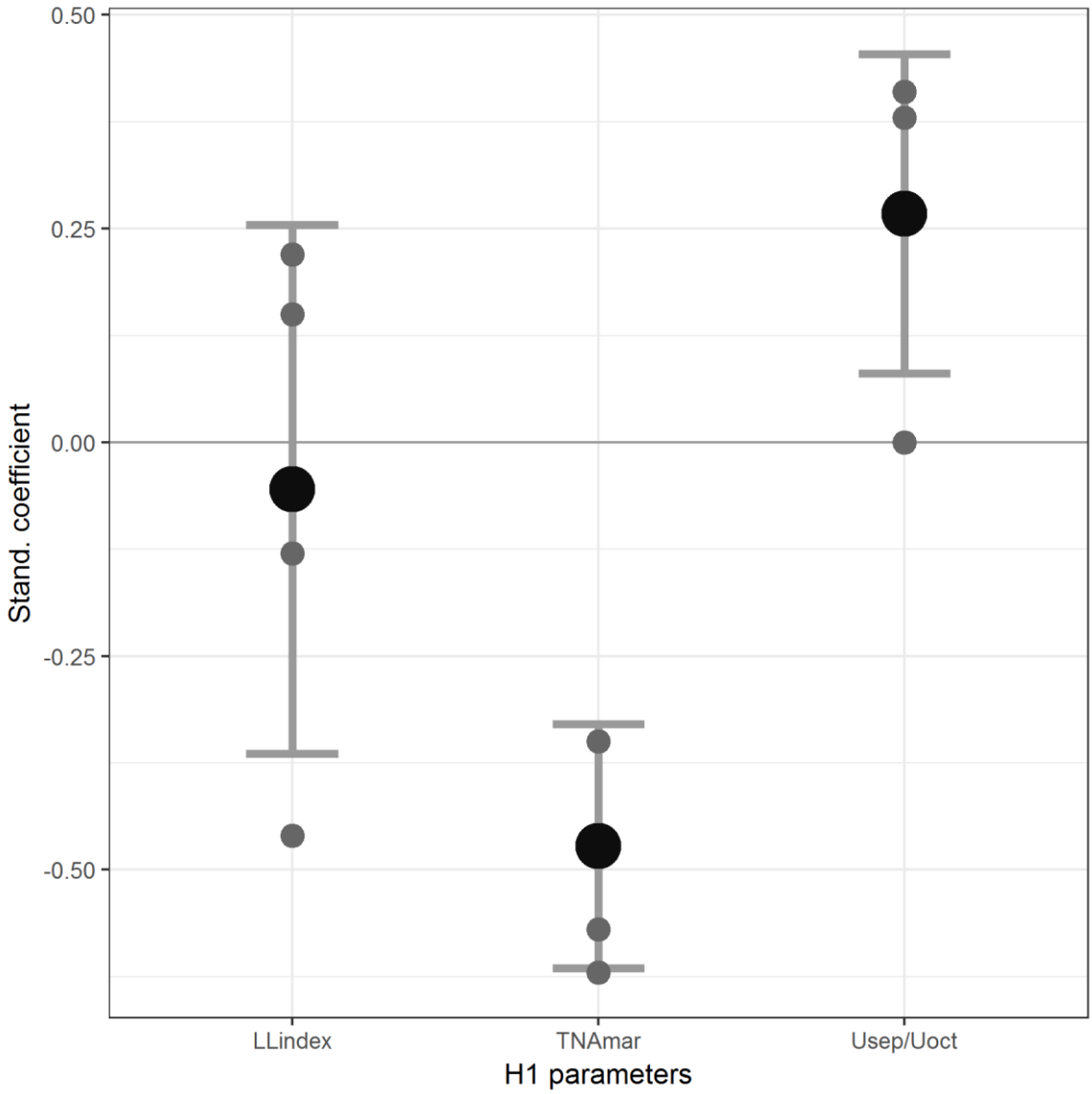

Fig. 5:

Variable importance plot for CPUE.kg, both raw and standardised, based on 4 models (Table 3).

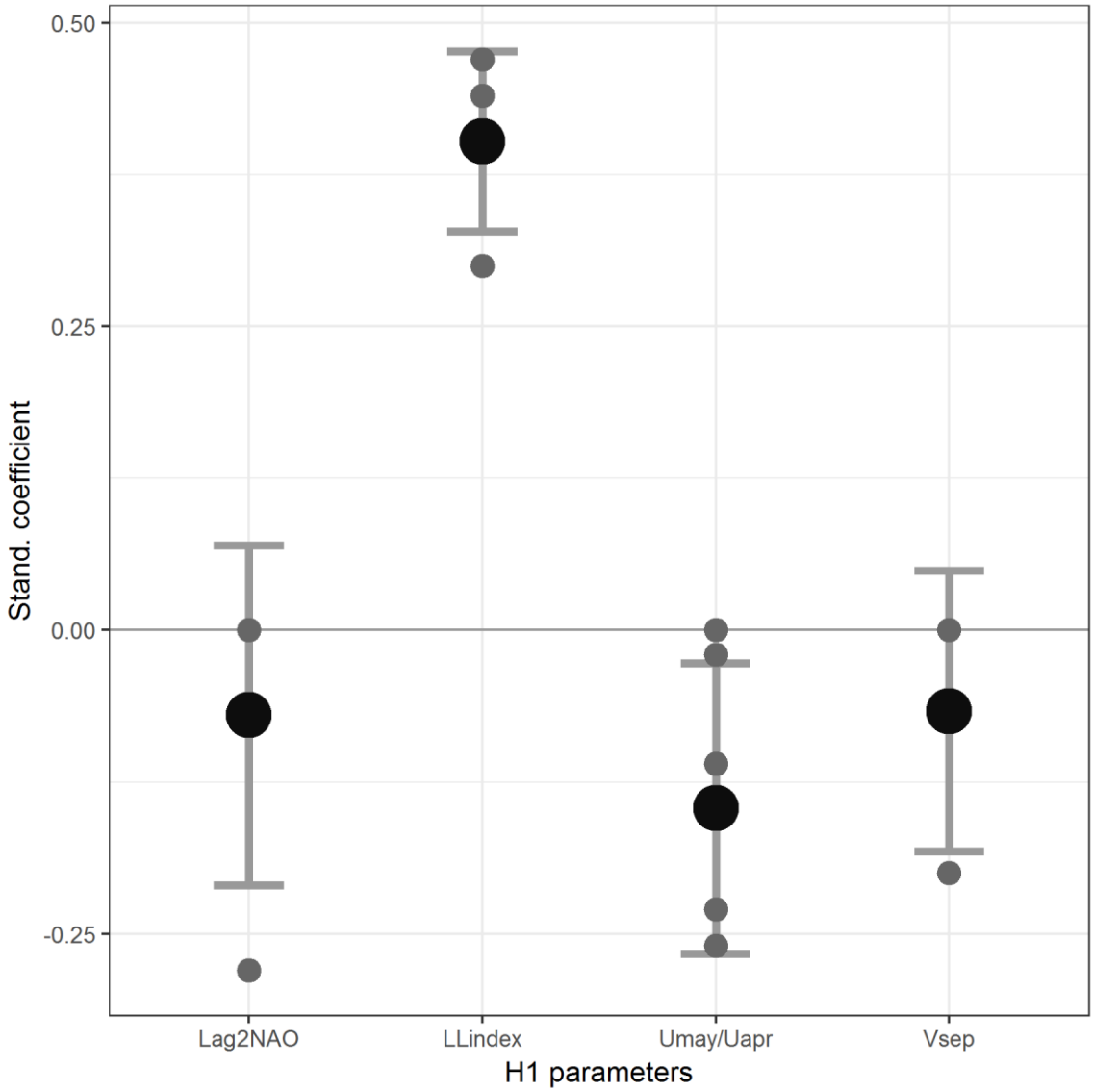

Fig. 6:

Variable importance plot for CPUE.nr, both raw and standardised, based on 4 models (Table 3).

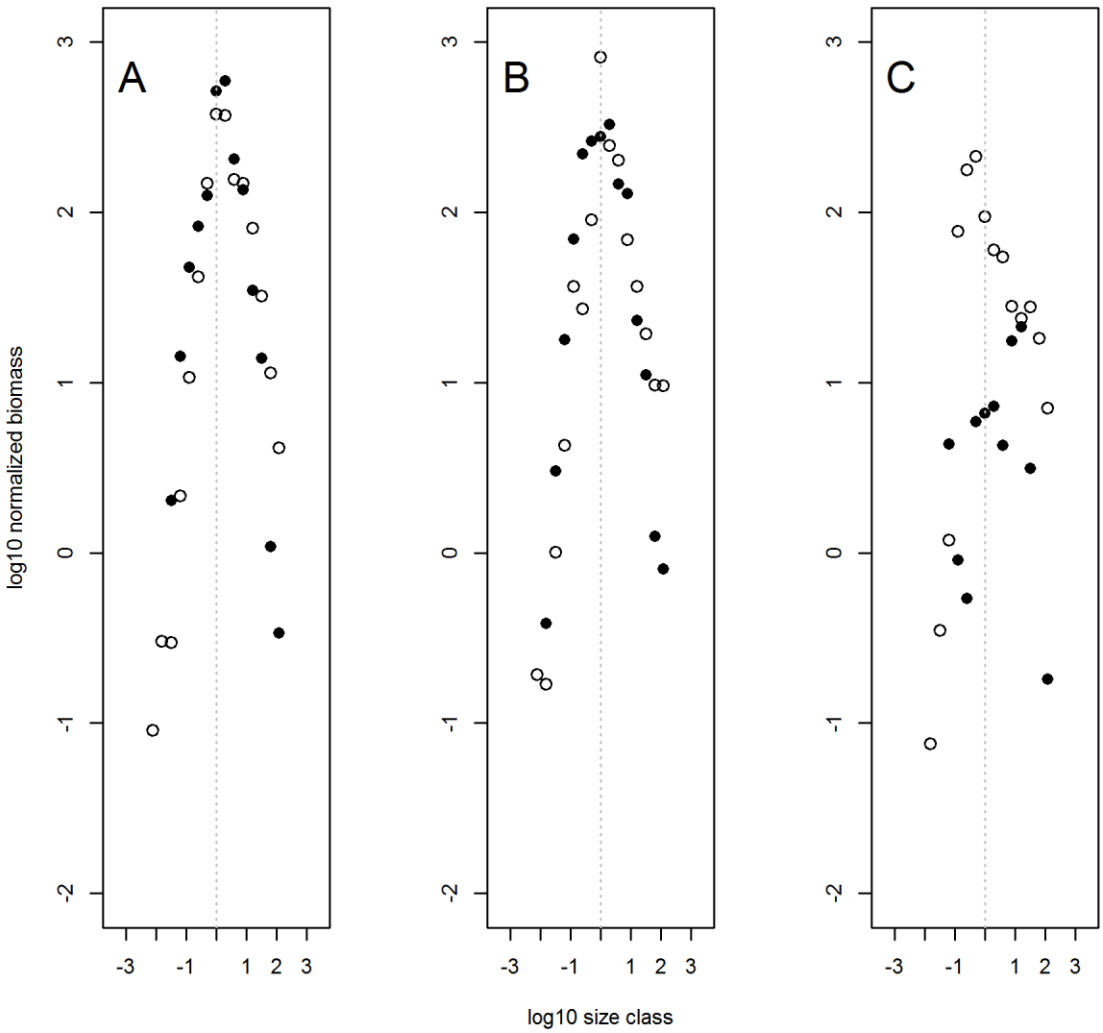

Fig. 7:

Biomass size distribution plots for historical (o) and 2015 data (•) by region. Vertical line indicates size class 2^0 g. (A) – tropics, (B)- subtropics, (C)- temperate.

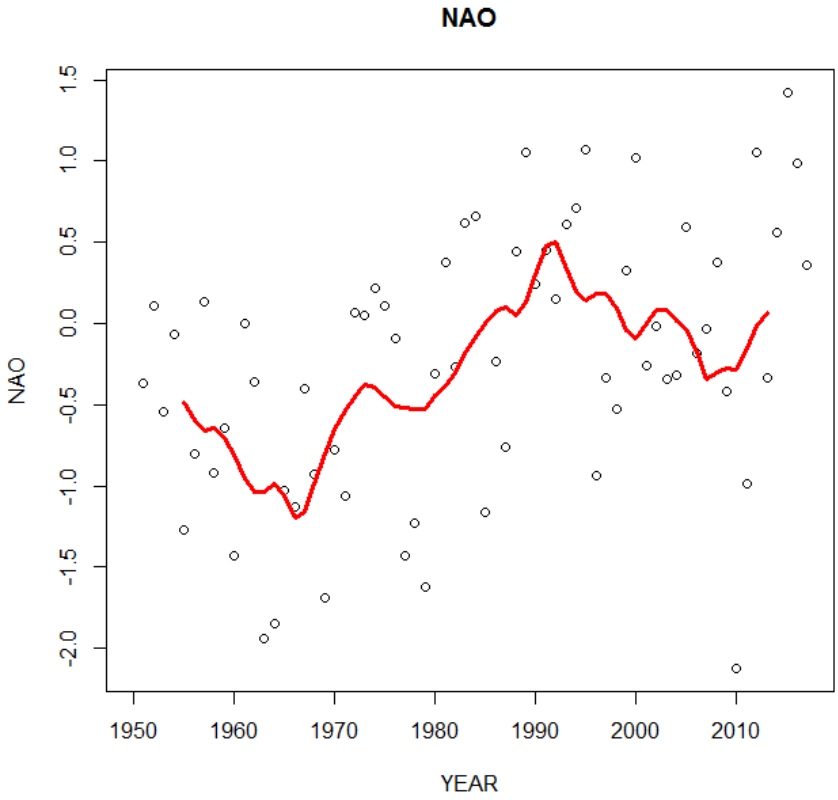

Fig. 8:

Time series of NAO and 8-yrs moving average shows that in the 1960's NAO was low and has increased until the 1990's with a small depression afterwards until 2009.

Appendix

QQ plots for models (CPUE.nr and CPUE.kg)

Report to model performance shown in Table 3.

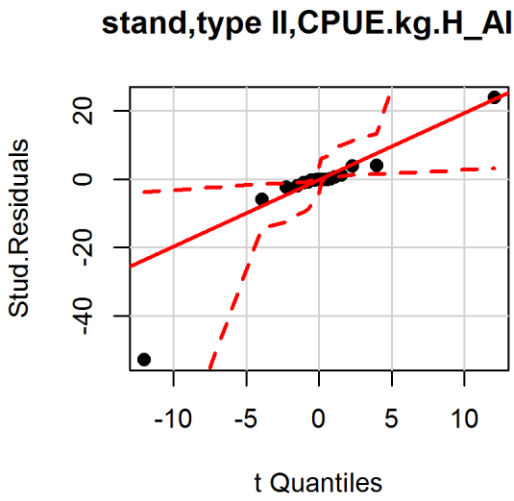

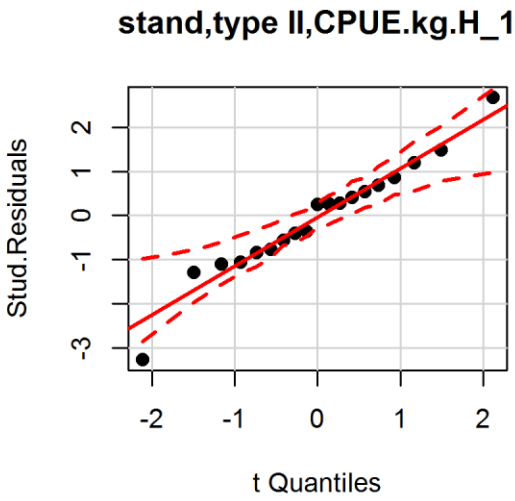

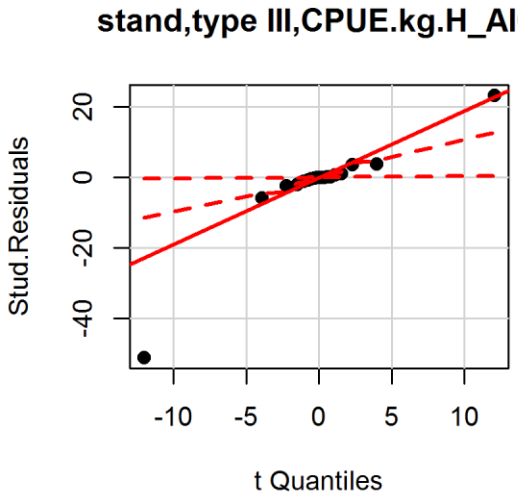

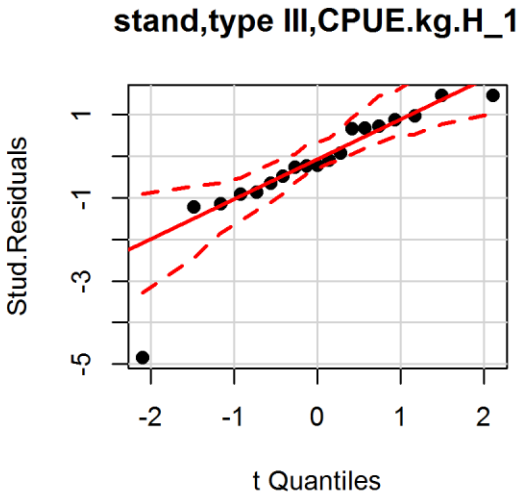

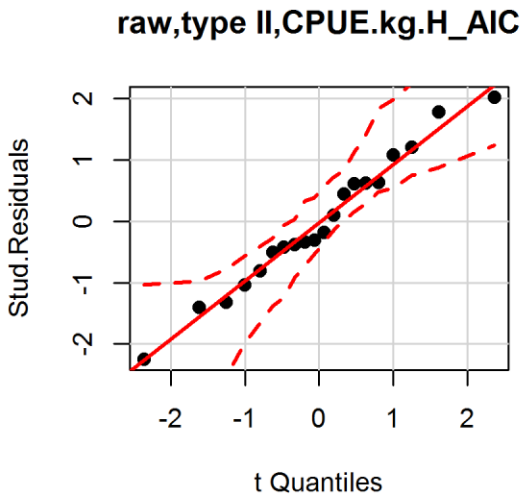
raw,type II,CPUE.kg.H_AIC
Stud.Residuals
t Quantiles

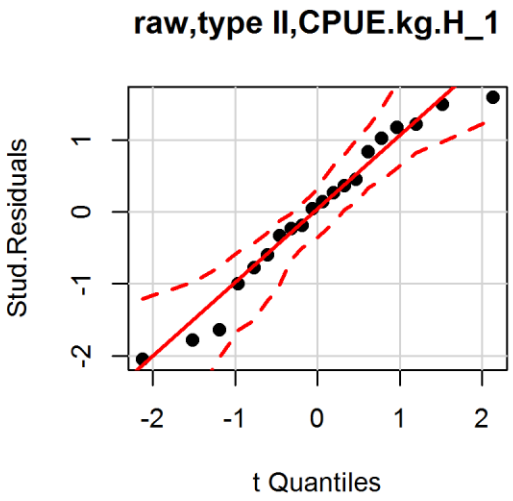
raw,type II,CPUE.kg.H_1
Stud.Residuals
t Quantiles

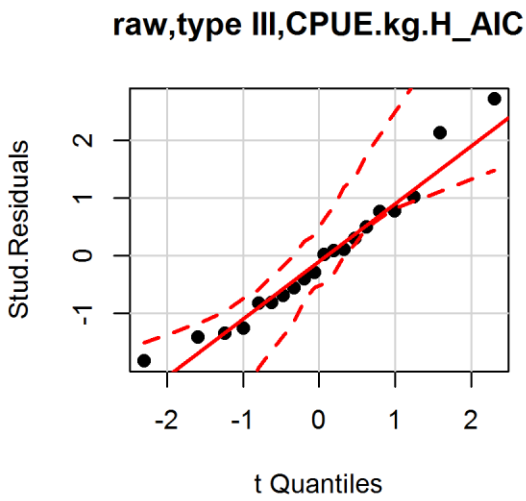
raw,type III,CPUE.kg.H_AIC
Stud.Residuals
t Quantiles

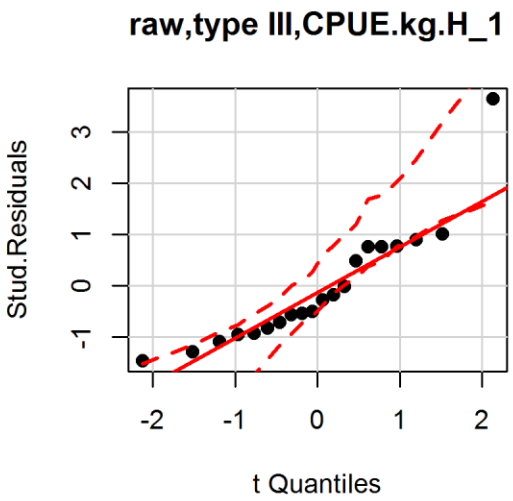
raw,type III,CPUE.kg.H_1
Stud.Residuals
t Quantiles

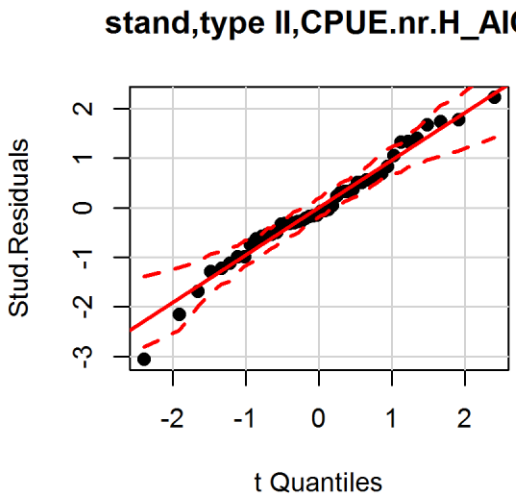
stand,type II,CPUE.nr.H_AIC
Stud.Residuals
t Quantiles

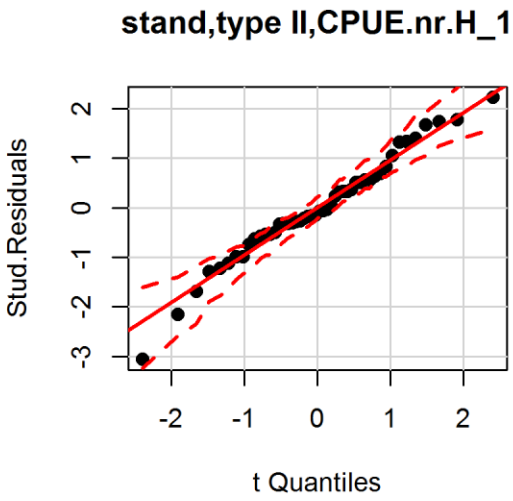
stand,type II,CPUE.nr.H_1
Stud.Residuals
t Quantiles

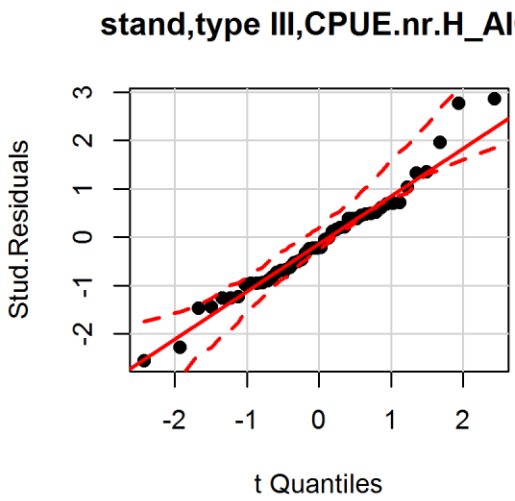
stand,type III,CPUE.nr.H_AIC
Stud.Residuals
t Quantiles

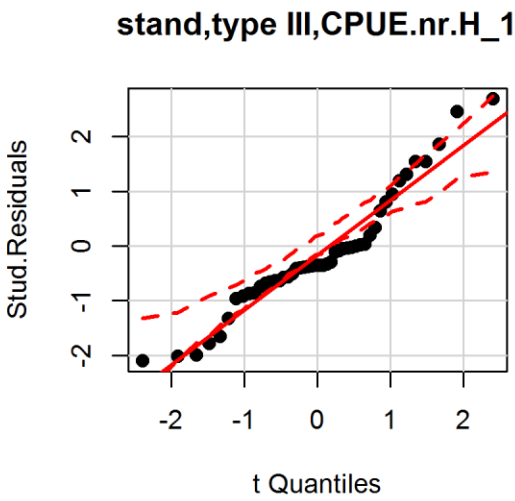
stand,type III,CPUE.nr.H_1
Stud.Residuals
t Quantiles

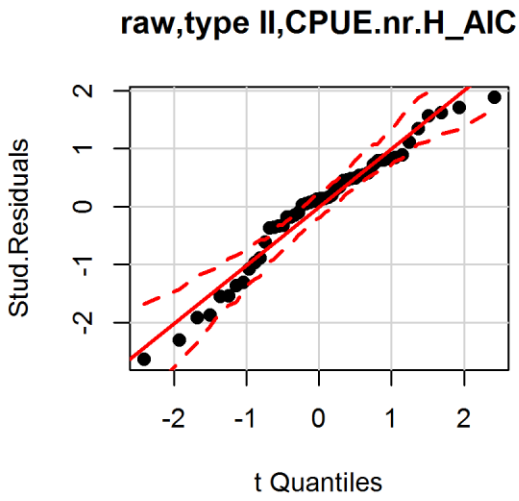
raw,type II,CPUE.nr.H_AIC
Stud.Residuals
t Quantiles

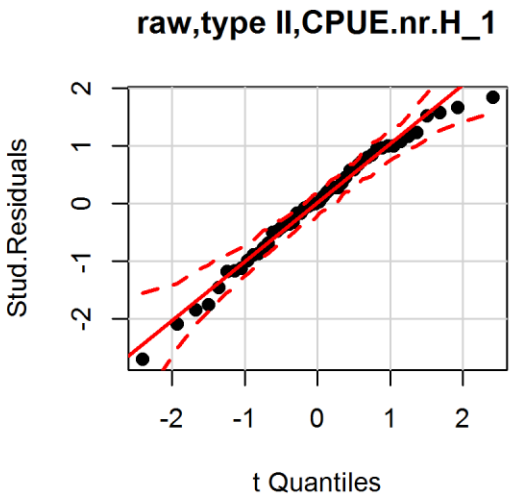
raw,type II,CPUE.nr.H_1
Stud.Residuals
t Quantiles

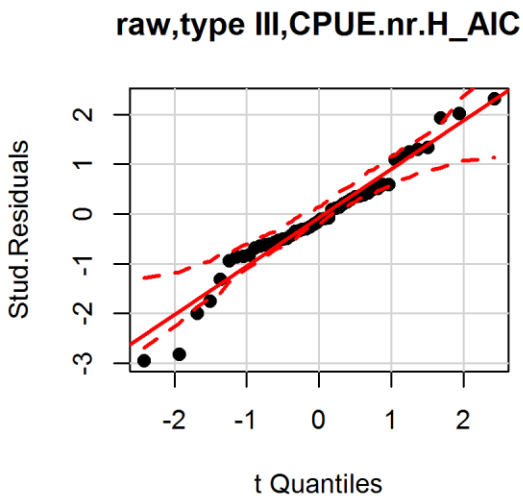
raw,type III,CPUE.nr.H_AIC
Stud.Residuals
t Quantiles

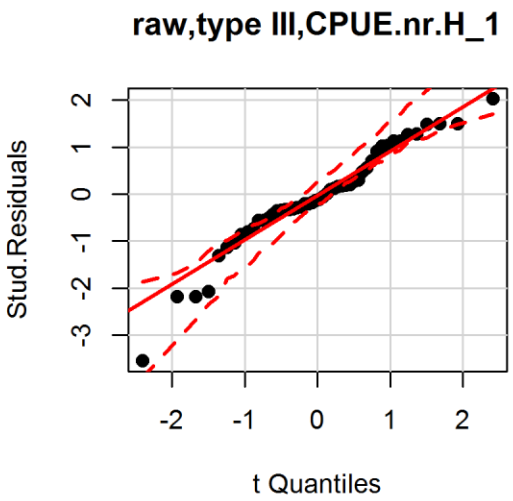
raw,type III,CPUE.nr.H_1
Stud.Residuals
t Quantiles